

Supplemental Figure 1: Dclk1-Cre & Dclk1-CreTM label long-lived epithelial tuft cells

A) Cloning strategy of Dclk1-CreGFP and Dclk1-CreERT mice and depiction of Cre-mediated recombination in Dclk1-CreERT mice following induction with Tamoxifen. **B)** LacZ staining of stomach tissue from Dclk1 R26LacZ mice at various time points post induction with Tamoxifen. **C&D)** Representative fluorescent photographs of small intestinal (C) and colonic (D) sections from 12 months old Dclk1-CreERT R26mTomatoGFP mice without administration of Tamoxifen. No recombination (as indicated by absence of membranous GFP) can be seen. **E&F)** Representative FACS plot of intestinal (E) and colonic (F) cell preparations from Dclk1 R26tdTom mice. Cells were gated based on red-fluorescence (Dclk1) and CD326 (EpCam) expression.

Supplemental Figure 2: Dclk1-Cre & Dclk1-CreTM labeled cells express tuft cell markers

A-C) Immunofluorescence for epithelial tuft cell markers (Dclk1, alpha-gustducin & acetylated tubulin) in the intestine (A), colon (B) and stomach (C) of Dclk1-CreGFP mice. **D)** Cox2 staining (red) on Dclk1 R26TGFP mice. **E)** Quantification of overlap between Cox2 and Dclk1 recombined cells in the small intestine of Dclk1 R26tdTom mice.

Supplemental Figure 3: Small intestinal Dclk1⁺ require neural input for survival

A) Small intestinal organoids from Dclk1 R26tdTom mice cultured in the presence of GFP positive neurons 5 days (left panel) and 10 days (right panel) after isolation. **B)** Quantification of Dclk1 cells in intestinal organoids in the presence and absence of neurons 10 days post isolation. **C-F)** Intestinal organoids derived from Dclk1 R26DTA mice cultured in the presence (D&F) and absence of neurons (C&E). 4OH-Tamoxifen was added to induce expression of DTA in Dclk1⁺ cells (C&E). **G)** Quantification of intestinal organoids in the presence and absence of neurons (left panel) and after Dclk1 cell ablation (right panel).

Supplemental Figure 4. Dclk1⁺ cells require proper innervation for survival

A) Immunohistochemistry of PGP 9.5 (left) and Dclk1 (right) on biopsy samples from intestinal transplant patients. Upper panels show samples from native, lower panels from graft intestine. **B)** Quantification of Dclk1 positive cells in biopsy samples (n=2) depicted

in A). **C**) Immunofluorescence for peripherin (green) on wildtype (left) and $RET^{-/-}$ mice (right) **D**) Immunofluorescence for Cox2 (red) on wildtype (left) and $RET^{-/-}$ mice (right). **E**) Quantification of intestinal tuft cells in wildtype and $RET^{-/-}$ mice.

Supplemental Figure 5: Gastric Dclk1+ cells require neural input for survival

A-D) Gastric organoids derived from Dclk1 R26tdTom mice cultured in the absence (A&C) and presence of neurons after 3 (A&B) and 14 (C&D) days in culture. Dclk1+ cells express tdTomato (red) neurons express GFP (green). **E**) Immunohistochemistry for Dclk1 on paraffin embedded gastric organoids in the absence (control) and presence of neurons (+nerve). Arrowheads mark Dclk1 positive cells. **F**) Quantification of Dclk1+ cells in gastric organoids in the presence of absence of neurons. **G&H**) Representative photographs of intestinal organoids derived from Dclk1-CreERT x R26tdTomato mice cultured in the presence (H) and absence of 100 μ M Pilocarpine (G). **I**) Quantification of Dclk1+ cells in (G) and (H).

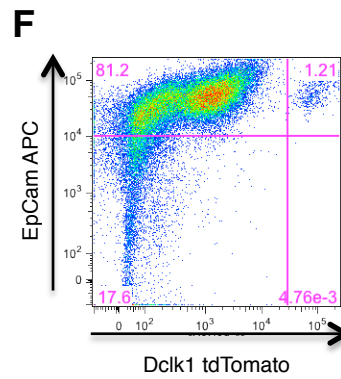
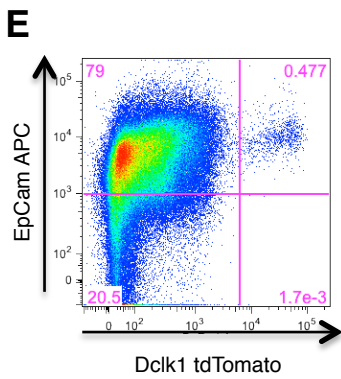
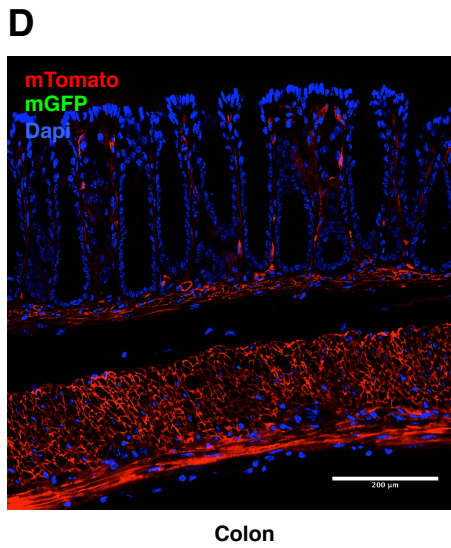
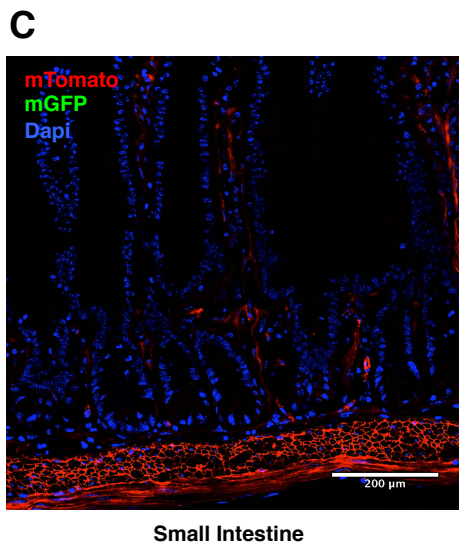
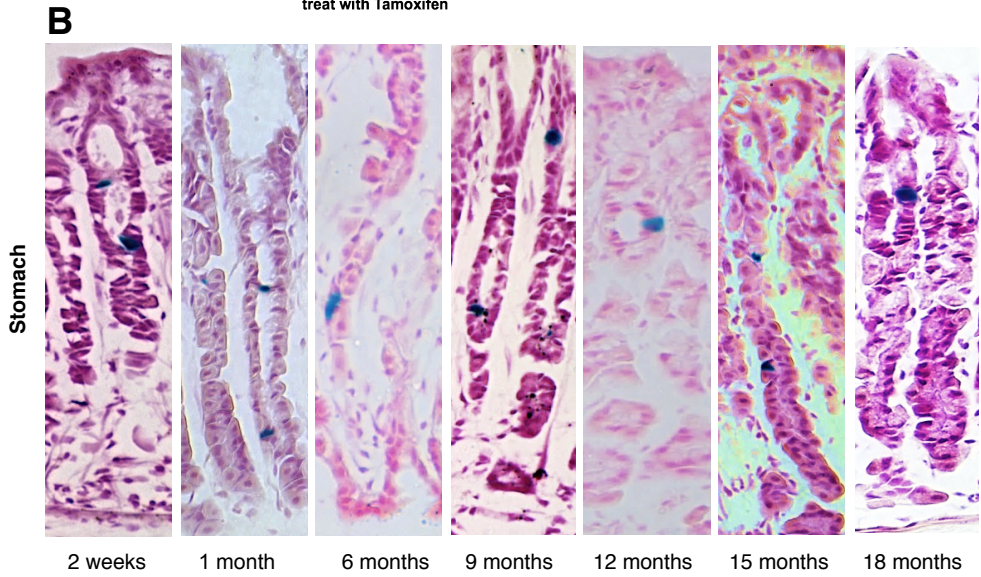
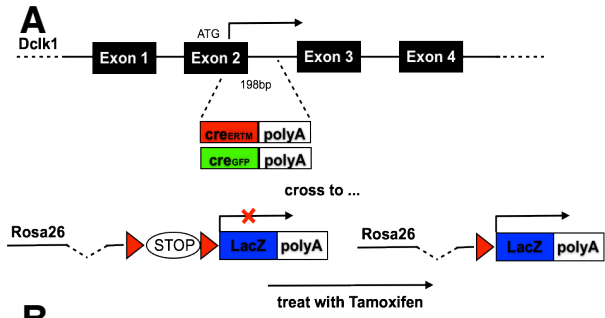
Supplemental Figure 6: Dclk1 cells expand in response to chronic inflammation and in preneoplastic states

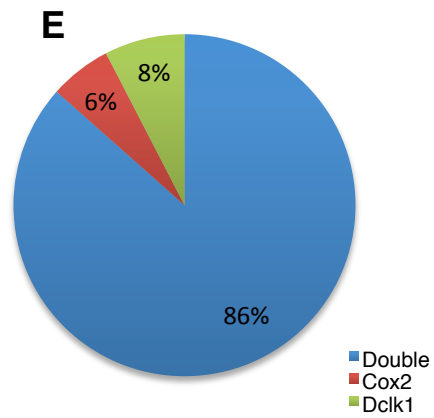
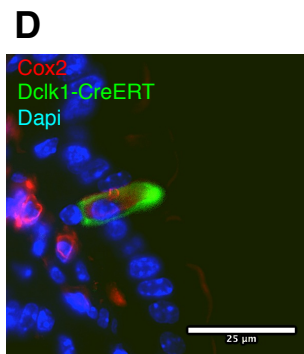
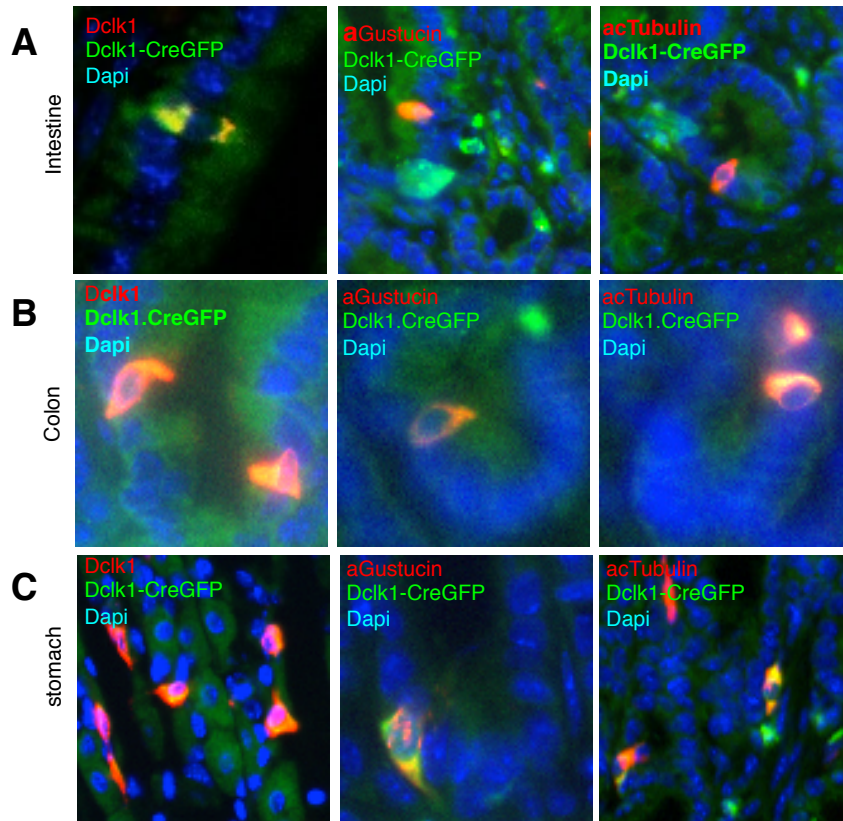
A) Immunohistochemistry for Dclk1 on the corpus of HKATPase-IL1 β mice infected with *H. felis*. **B**) Immunohistochemistry for Dclk1 Barrett's lesions in P2-IL1 β mice. **C&D**) Immunofluorescence for Dclk1 on intestinal sections from B6 mice infected with *H. hepaticus* (D) and controls (C). **E**) Quantification of Dclk1+ cells in mice infected with *H. hepaticus* and controls. **F&G**) Immunohistochemistry for Dclk1 on colonic sections from mice infected with *B. fragilis* (G) and controls (F). **H**) Quantification of Dclk1+ cells in (F&G) (Scale bars: 50 μ m).

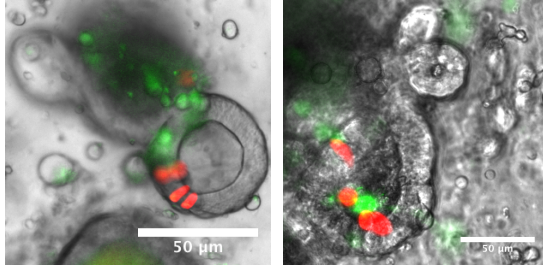
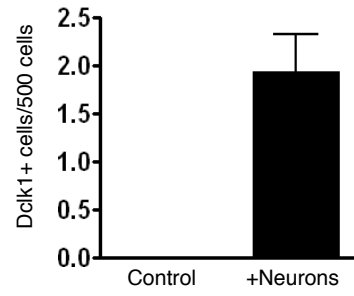
Supplemental Figure 7: Pathology of murine models of colonic neoplasia

A) Early colonic polyps in APC^{min} mice. Proliferation with evidence of surface maturation is seen. An early sessile proliferative lesion is characterized by increase in proliferative zone of polyp in (A). Right panel: Typical early polypoid proliferative lesion. **B**) H&E of colonic lesions in Lgr5-CreERT x APC^{flox/flox} mice: Numerous colonic adenomas are present. Left panel: Numerous small adenomas with low grade dysplasia arising in the background of colonic mucosa with multifocal low grade dysplasia Right panel: Higher power magnification shows minute adenoma composed of two dysplastic crypts.

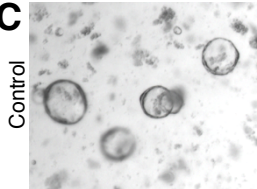
C) H&E of colonic lesions in Dclk1-CreERT x APC^{fl^{ox}/fl^{ox}}: Few adenomas are present with features of invasive carcinoma and complex architectural patterns of growth and associated desmoplastic stroma. Left panel: A large advanced polyp with marked architectural complexity arising in the background of normal mucosa Right panel: Higher power magnification shows complex cribriform structures associated with focal tumor cell necrosis. The surrounding fibroblastic tissue reaction characterizing desmoplasia surrounding the neoplastic epithelium is a feature of invasive carcinoma (Original magnifications 40x, 200x)



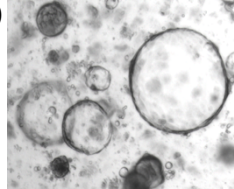


A**B**

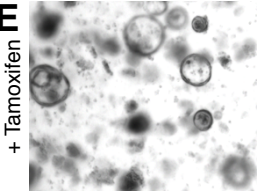
Dclk1 CreERT x R26DTA

C

Control

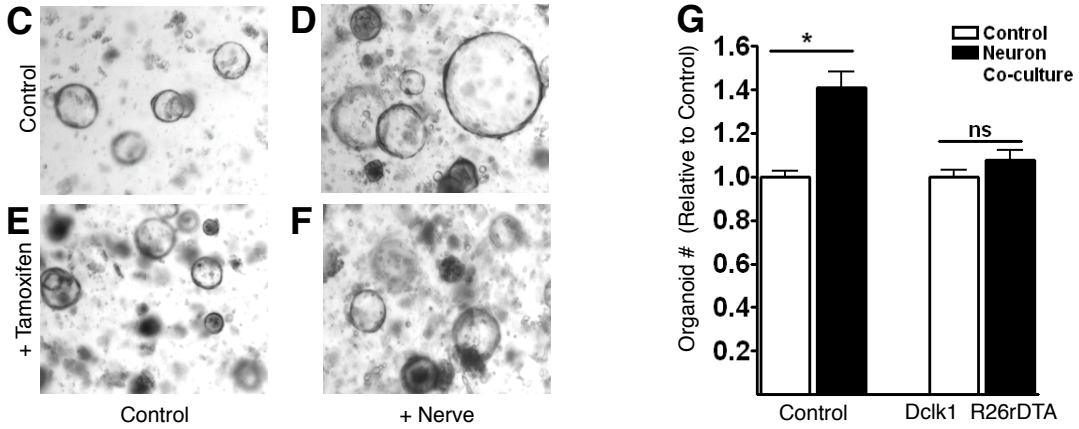
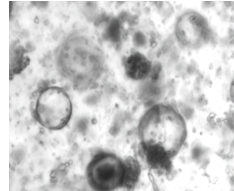
D

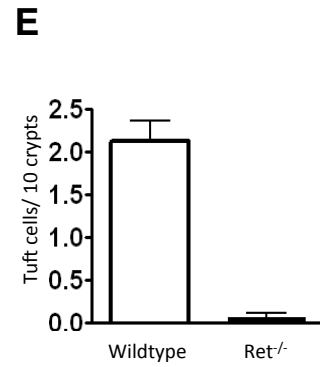
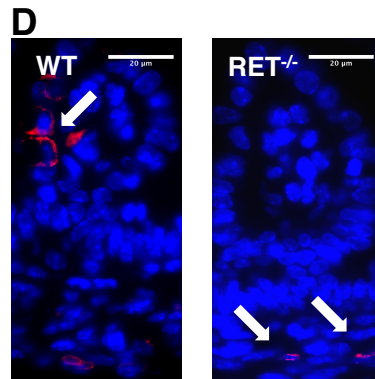
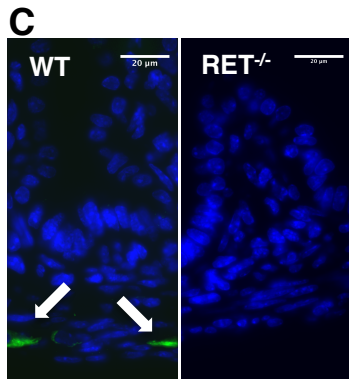
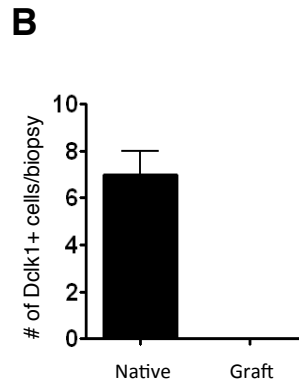
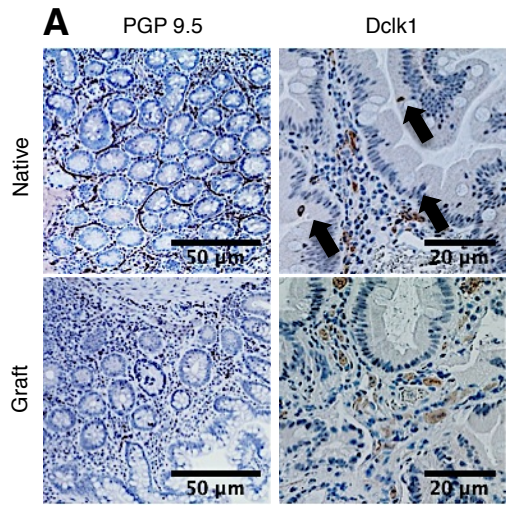
+ Nerve

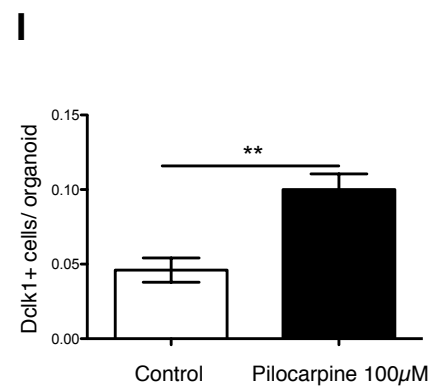
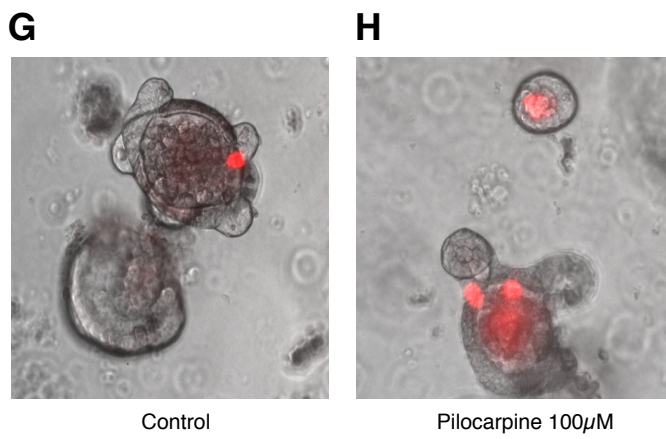
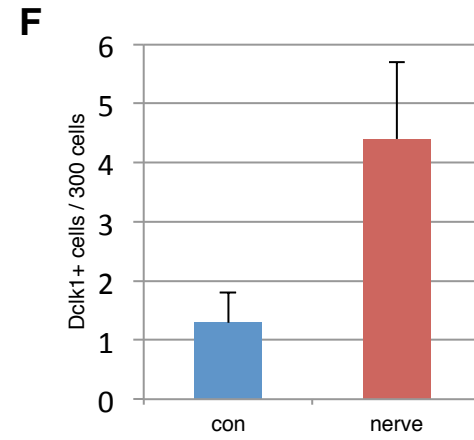
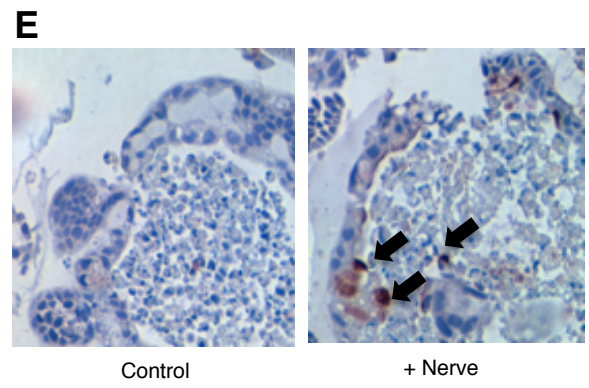
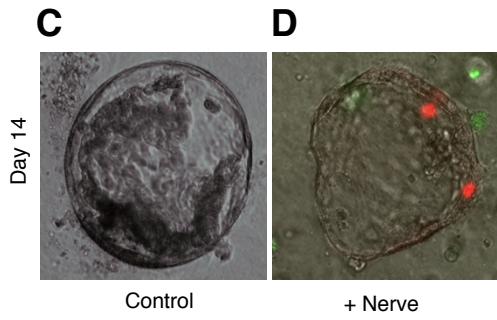
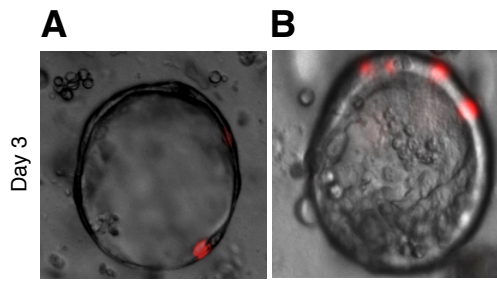
E

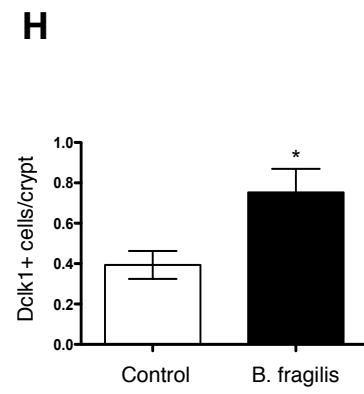
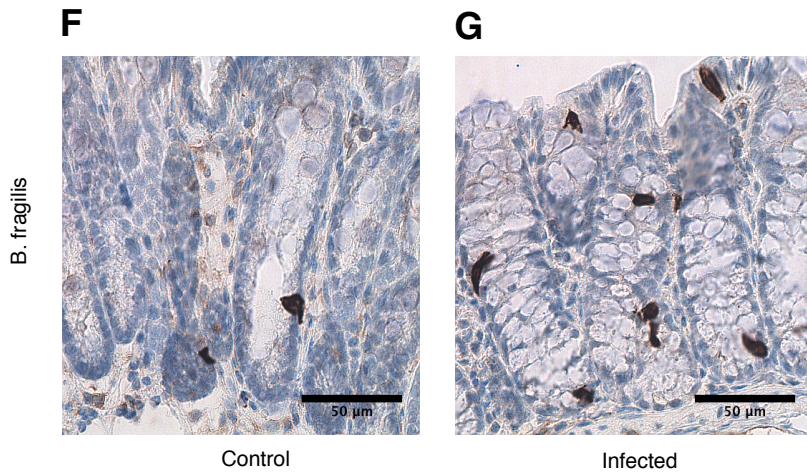
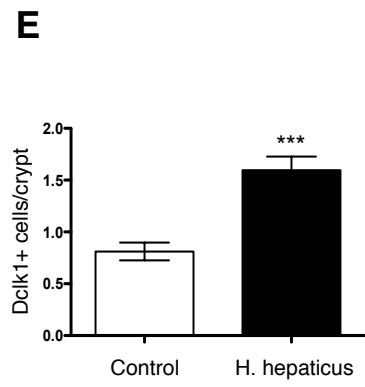
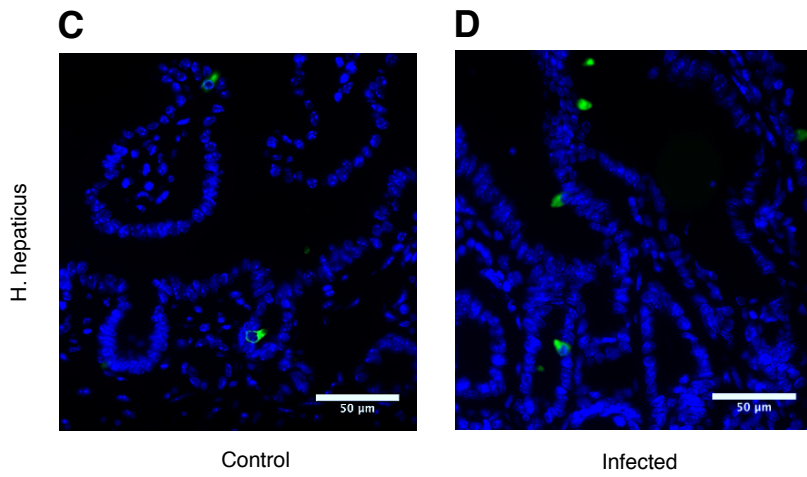
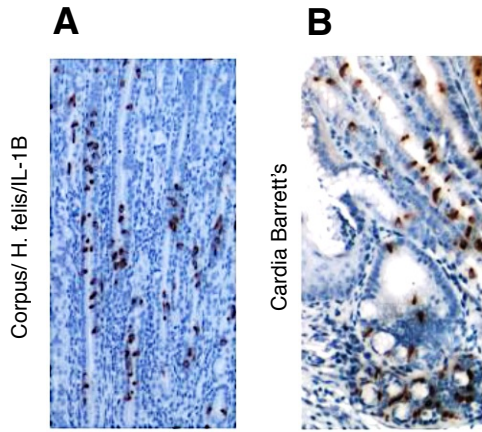
+ Tamoxifen

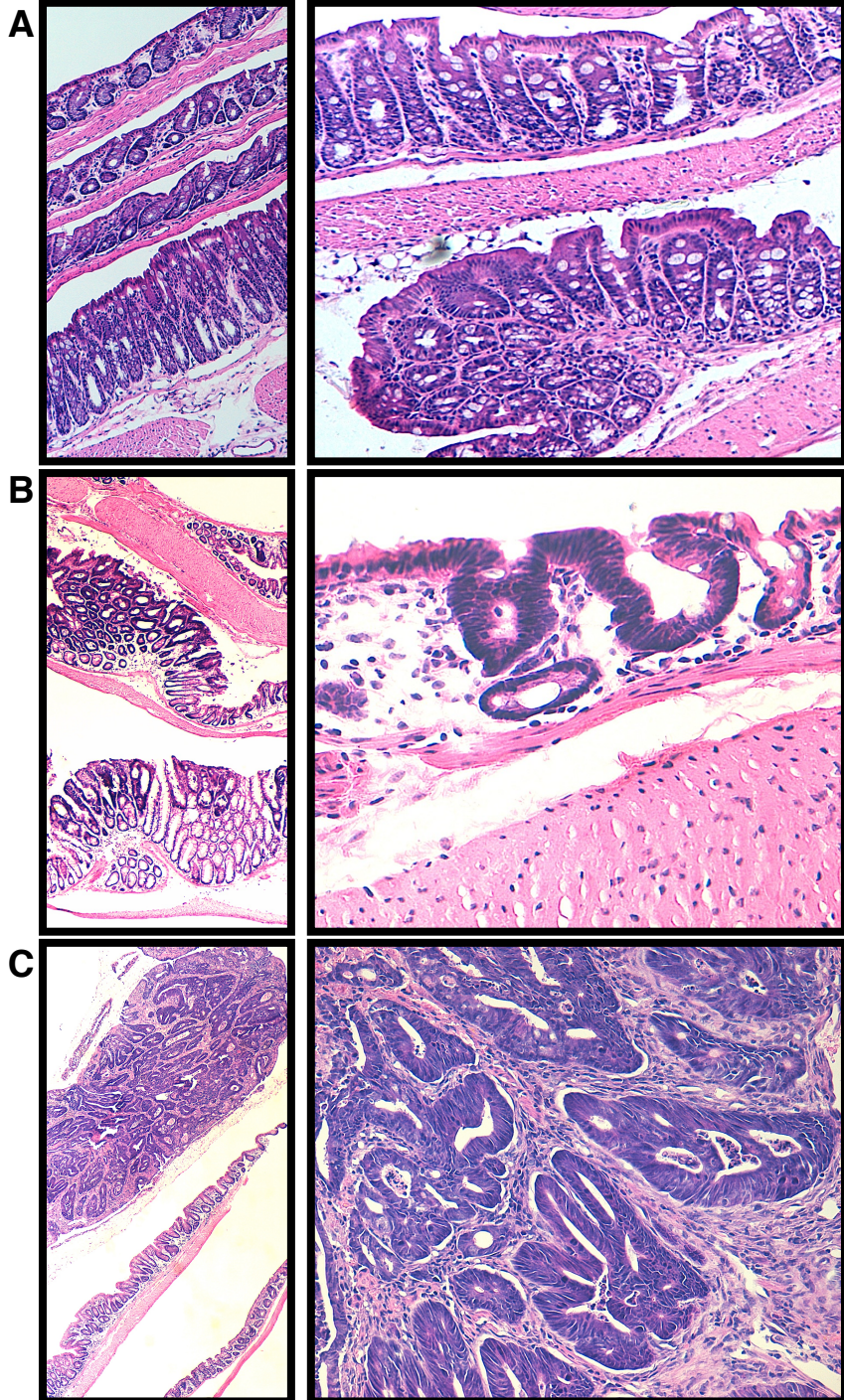
Control

F









Supplemental Table 1: Immunohistochemical analysis of recombined cells in Dclk1-Cre & CreERT mice

| Dclk1-CreTM | x | Recombined cells (100 crypts) | Dclk1 | aGustducin | acTubulin | ChromA |
|-------------------------------|----------|--------------------------------------|--------------|-------------------|------------------|---------------|
| Corpus | | 42 | 95% ±2% | 81% ±4% | 98% ±1% | 0% ±0% |
| Antrum | | 54 | 98% ±2% | 89% ±2% | 97% ±2% | 5% ±0% |
| Small Intestine | | 169 | 96% ±2% | 79% ±5% | 93% ±2% | 3% ±1% |
| Colon | | 81 | 98% ±2% | 94% ±2% | 98% ±2% | 0% ±0% |
| Dclk1-CreGFP | | GFP+ cells (100 crypts) | Dclk1 | aGustducin | acTubulin | ChromA |
| Corpus | | 56 | 85% ±4% | 72% ±4% | 82% ±5% | 1% ±0% |
| Antrum | | 61 | 87% ±7% | 74% ±2% | 83% ±5% | 2% ±1% |
| Small Intestine | | 190 | 81% ±12% | 59% ±4% | 81% ±5% | 1% ±0% |
| Colon | | 108 | 82% ±6% | 61% ±7% | 85% ±4% | 1% ±0% |

Supplemental Table 2: Mouse strains used in the manuscript

| Full Name | Abbreviation | Source | Consensus Name |
|--------------------------------|---------------------|---------------|---|
| APC ^{flox/flox} | | NCI | B6: Apctm2Rak |
| C57BL/6J | B6 | Jackson labs | C57BL/6J |
| DCLK1-CreERT | Dclk1 | Generated | DCLK1-BAC-CreERT |
| DCLK1-CreGFP | | Generated | DCLK1-BAC-CreGFP |
| Dclk1 ^{floxed/floxed} | | Jackson labs | Dclk1tm1.2Jgg/J |
| Rosa26 DTA | R26DTA | Jackson labs | B6.129P2-Gt(ROSA)26Sortm1(DTA)Lky/J |
| Rosa26 LacZ | R26LacZ | Jackson labs | 129S-Gt(ROSA)26Sortm1Sor/J |
| Rosa26 mTomato/mGFP | R26-TGFP | Jackson labs | B6.129(Cg)-Gt(ROSA)26Sortm4(ACTB-tdTomato,-EGFP)Luo/J |
| Rosa26 tdTomato | R26tdTom | Jackson labs | B6;129S6-Gt(ROSA)26Sortm9(CAG-tdTomato)Hze/J |
| Rosa26DTR | R26iDTR | Jackson labs | CBy.B6-Gt(ROSA)26Sortm1(HBEGF)Awai/J |
| UBC-GFP | | Jackson labs | C57BL/6-Tg(UBC-GFP)30Scha/J |

Supplemental Table 3: Antibodies used in the manuscript

| Name | Company | Order Number | Dilution |
|---|----------------|---------------------|-----------------|
| Alexa Fluor 488 (F(ab') ₂ Goat-anti-Rabbit | Invitrogen | A11070 | 1:500 |
| Alexa Fluor 488 Conjugate anti-GFP | invitrogen | A21311 | 1:50 |
| Alexa Fluor 546 Donkey-anti-mouse | Invitrogen | A10036 | 1:500 |
| Alexa Fluor 546 Donkey-anti-Rabbit | Invitrogen | A10040 | 1:500 |
| anti-acetylated-Tubulin | Sigma-Aldrich | T7451 | 1:100 |
| anti-alpha-Gustducin | Santa Cruz | sc-395 | 1:200 |
| anti-BrdU | AbCam | ab6326 | 1:100 |
| anti-Cox2 | Pierce | PA1-20955 | 1:250 |
| anti-Dcamk1 | Abgent | AP7219b | 1:200 |
| anti-Ki67 | abcam | ab15580 | 1:500 |
| anti-Muc2 | Santa Cruz | sc-15334 | 1:500 |
| anti-NGF | Santa Cruz | sc-549 | 1:100 |
| anti-Peripherin | Millipore | AB1530 | 1:200 |
| anti-β-catenin | BD Bioscience | 610157 | 1:100 |
| anti-β-Gal | AbCam | ab9361 | 1:1000 |
| anti-TFF3 | Santa Cruz | sc-28927 | 1:500 |